



# Effects of solutioning and ageing treatments on properties of Inconel-713C nickel-based superalloy under creep loading

Mahboobeh Azadi<sup>a</sup>, Armin Marbout<sup>b</sup>, Sama Safarloo<sup>a</sup>, Mohammad Azadi<sup>b,\*</sup>, Mehdi Shariat<sup>a</sup>, Mohammad Hassan Rizi<sup>b</sup>

<sup>a</sup> Faculty of Materials and Metallurgical Engineering, Semnan University, Semnan, Iran

<sup>b</sup> Faculty of Mechanical Engineering, Semnan University, Semnan, Iran

## ARTICLE INFO

### Keywords:

Nickel-based superalloy  
Inconel 713C  
Solutioning effect  
Ageing effect  
Creep behavior  
Microstructure  
Fracture surface

## ABSTRACT

As nickel-based superalloys have been widely used in turbine blades of turbo-chargers in automobile industries, this article has presented the creep behavior of the Inconel-713C nickel-based superalloy. For this objective, forced-controlled creep testing has been performed at the temperature of 850 °C and under the stress of 585.5 MPa. Then, the effect of the solutioning process on creep (time-dependent) properties of the superalloy was investigated. Optical and scanning electron microscopies were utilized to study the material microstructure, before and after creep testing. The X-ray diffraction (XRD) spectrometry was also used to detect different phases in the superalloy. Results showed that solutioning at 1200 °C for 1 h had a lowering effect on the creep rupture time of the Inconel-713C superalloy, as the mean size of the  $\gamma'$  particles crystallite was about 6.8 nm. When the superalloy was aged for 16 h at 930 °C, an insignificant effect with respect to the as-cast sample could be observed, due to the precipitation of NbC carbides (at grain boundaries) and the coarsening behavior of  $\gamma'$  particles. Consequently, different microstructures led to different creep fracture mechanisms for this alloy. The decomposition of MC carbides to  $M_{23}C_6$  was also observed for all samples after creep testing.

## 1. Introduction

Nickel-based superalloys have been widely used in different applications, where require high strengths at high temperatures. Most types of these superalloys are age-hardenable, as they have  $\gamma'$  particles with the chemical composition of  $Ni_3(Al,Ti)$  in the matrix of the  $\gamma$  phase. Properties of the superalloy depend on the size and the distribution of  $\gamma'$  precipitates [1–3]. A uniform distribution of the precipitating phase improves significantly mechanical properties, such as the tensile strength, the fatigue lifetime, the creep rupture strength, etc. [4,5]. Several researches have investigated about the heat treatment process (including solutioning and ageing) of different nickel-based superalloys. More details of the literature reviews on this topic can be found in following paragraphs.

Zhao et al. [1] analyzed  $\gamma'$  coarsening and age-hardening behaviors in a nickel-based superalloy. They showed that precipitates of such alloy with a standard precipitation treatment, contained  $\gamma'$ , MC, and  $M_{23}C_6$ . Due to the different growth rates of  $\gamma'$  precipitates, the micro-hardness of the alloy decreased significantly by increasing the ageing temperature. Li et al. [2] investigated coarsening and age hardening behaviors of  $\gamma'$  precipitates in the GH742 alloy. Their micro-hardness

studies depicted that increasing the ageing temperature from 900 °C to 1050 °C decreased the hardness of the material, which was depended on the  $\gamma'$  critical particle size. Mostafaei et al. [6] studied the effect of solutioning and ageing heat treatments on the microstructure and mechanical properties of the powder bed binder jet printed 625 nickel-based superalloy. Their results indicated that the ageing process resulted in the formation of intermetallic phases, such as  $Ni_3Nb$  and  $Ni_2(Cr,Mo)$  and carbides, such as NbC and  $Cr_{23}C_6$  in the microstructure. Although the micro-hardness and the tensile strength of aged specimens increased, the ductility value decreased. Whitmore et al. [7,8] investigated the effect of single and double ageing processes on the Inconel-718 nickel-based superalloy. They found that the double ageing treatment led to increase the hardness, as compared to the single ageing treatment. A dense dispersion of  $\gamma'$  phase clusters with the size of 1–2 nm was observed after both single and double ageing processes.

Singh et al. [9] reported effects of the microstructure and the temperature on the crussard-jaoul work hardening coefficient, in the aged 625 alloy. They claimed that coarse particles exhibited the anomalous hardening behavior at elevated temperatures. Joseph et al. [10] studied the microstructure and mechanical properties of the Haynes-282 Nickel-based superalloy, when the alloy was heat treated under

\* Corresponding author.

E-mail address: [m\\_azadi@semnan.ac.ir](mailto:m_azadi@semnan.ac.ir) (M. Azadi).

different conditions. Their results demonstrated that the coarser  $\gamma'$  phase resulted in a reduction in the strength level. Besides, inter-connected carbides led to the brittle fracture with a 50% reduction in the ductility. Jun et al. [11] investigated heat treatment regimes on the microstructure and creep properties of FGH95 superalloy. Their results indicated that under the applied stress of 1034 MPa and at the temperature of 650 °C, the alloy (that cooled in the molten salt) had the better creep resistance. Nortershauser et al. [12] compared the creep behavior of specimens, loaded in [001] and [110] directions. They showed that creep specimens loaded in the [110] direction had lower minimum creep rates, significantly.

As a conclusion on the literature review, still there is a lack of sciences about the creep behavior of superalloys, especially the Inconel-713C nickel-based superalloy. Although several articles [13–15] focused on the microstructure of the cast Inconel-713C nickel-based superalloy, the number of researches about creep behaviors of the mentioned material is still rare. Therefore, this article has included a study on properties of the mentioned material, under creep loading. It should be noted that different conditions of creep testing for the Inconel-713C nickel-based superalloy have been previously performed and reported in the literature [16]. Then, this research has been perused the relation between the heat treatment and time-dependent properties of the material. Furthermore, as both solutioning and precipitation strengthening are major factors in strengthening mechanisms [17], the heat treatment procedure of the Inconel-713C nickel-based superalloy has been divided into the solutioning treatment and the ageing treatment. In addition, the behavior of these samples has been investigated under creep testing. The microstructural evaluation has been also done by optical and scanning electron microscopies.

## 2. Materials and experiments

In this research, the studied material was chosen as the Inconel-713C nickel-based superalloy. This alloy has been widely used in turbine blades of turbo-chargers in automotive industries [16,18]. The chemical composition (wt%) of the used alloy was measured as C: 0.12%, Cr: 14.00%, Nb + Ta: 1.91%, Ti: 0.97%, Al: 5.50%, Fe: 0.13%, Mn: 0.04%, Si: 0.45%, Zr: 0.06%, B: 0.01%, Mo: 4.50%, Cu: 0.01% and balance Ni.

The first sample was the as-cast product of the mentioned material. The second sample was solutionized at 1200 °C for 1 h and then, was cooled or quenched by the air. It should be noted that a high temperature was considered for the solutioning process, since it was found that some phases and carbides could not be solved under 1032 °C [17]. For the third sample, after solutioning, the ageing process was carried out in 930 °C for 16 h. More details of the heat treatment procedure is shown in Fig. 1.

After preparing different cylindrical specimens, they were tested by the forced-controlled tensile creep testing machine. Creep testing was

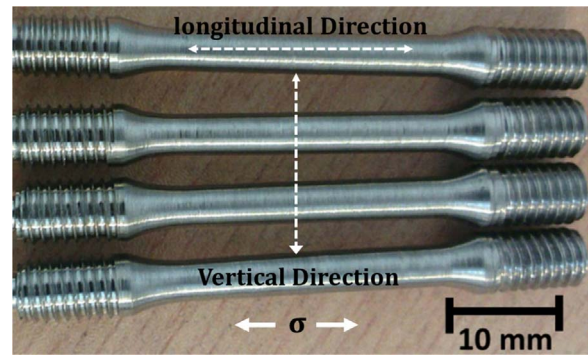


Fig. 2. The direction of the applied stress in creep testing on real specimens.

done according to ASTM-E139-11 [19]. More details of this test machine and the specimen geometry can be found in the literature [16]. According to test conditions, samples were heated at 850 °C and were forced under 585.8 MPa of the applied stress, at a constant load condition. The test was carried out by the Santam Company SCT-300 creep testing machine. For a better comparison, the applied stress and the temperature were constant for all specimens during creep testing. The cylindrical specimen is depicted in Fig. 2, with the direction of loading. It should be noted that only one creep test has been performed for each condition. As reported before, the repeatability of creep testing indicated a small deviation in results of the lifetime and the minimum strain rate [16]. Therefore, the uncertainty of results in creep testing was small for the studied material [16].

Before and after creep testing, samples were metallographically polished up to a 2000-grit surface finish, using SiC papers. Then, they were chemically etched in a fresh solution of the marble etchant, containing HCl, CuSO<sub>4</sub>, and H<sub>2</sub>O, for 3 s. Images by the optical microscope (OM) and the scanning electron microscope (SEM) were used to examine the microstructure. In addition, creep fractured surfaces of specimens were observed using the SEM. The mean radius of the  $\gamma'$  precipitates crystallite and the existent of different phases were examined using the X-ray diffraction (XRD) spectrometer. A CuK $\alpha$  radiation was used for this test and curves were recorded at a scanning rate of 0.0258 s<sup>-1</sup> with 2 $\theta$  (Bragg angle) scan range, from 10 to 90 degree. The Scherer equation [20] was utilized in this article to measure the size of the  $\gamma'$  particles crystallite. In this equation, the full-width at the half-maximum (FWHM) of the Bragg peak was used, as follows,

$$L = \frac{k\lambda}{B_m \cos\theta} \quad (1)$$

where  $L$  is the grain size,  $B_m$  is the FWHM of the Bragg peak,  $\lambda$  is the wavelength of X-ray,  $k$  is the dimensionless shape factor (with the value of 0.9) and  $\theta$  is the Bragg reflection angle [21].

## 3. Results and discussions

As a first result before creep testing, microstructures of the studied alloy in as-cast, solutionized and solutionized/aged states are shown in Fig. 3. The  $\gamma'$  participate and carbides were distributed in the  $\gamma$  matrix for the as-cast sample. The maximum length of carbides was as high as 150  $\mu$ m, observing in Fig. 3(a). The amount of  $\gamma'$  participates and carbides in the solutionized sample decreased, as shown in Fig. 3(b). Most of  $\gamma'$  participates were solutionized at 1200 °C in the  $\gamma$  matrix and a small amount of them retained in carbide branches. The length of carbides in the alloy decreased to 100  $\mu$ m or lower and their thickness lowered, too. The high temperature of solutioning (about 1200 °C) did not cause to dissolve all carbides, as also the other research [17] claimed. Kuo et al. [17] reported that the solutioning heat treatment, even higher than 1177 °C, did not dissolve all carbides. For the aged sample, the microstructure changed, shown in Fig. 3(c) and (d), and the

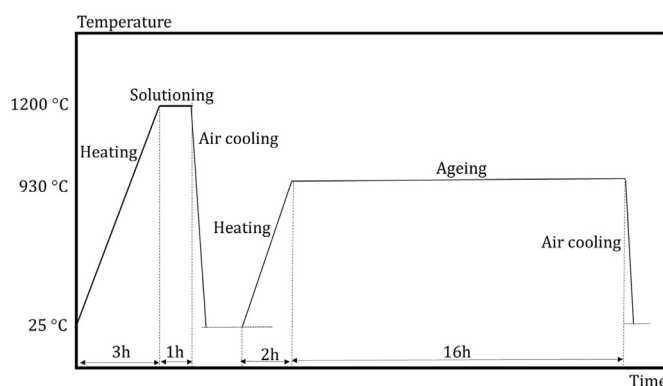


Fig. 1. The heat treatment procedure.

Download English Version:

<https://daneshyari.com/en/article/7974217>

Download Persian Version:

<https://daneshyari.com/article/7974217>

[Daneshyari.com](https://daneshyari.com)